

Cosmological Effects of Scalar-Photon Couplings: Dark Energy and Varying- α Models

A. Avgoustidis,^a C. J. A. P. Martins,^b A. M. R. V. L. Monteiro,^{b,c,d} P. E. Vielzeuf,^{b,c} G. Luzzi^e

^aSchool of Physics and Astronomy, University of Nottingham, University Park, Nottingham NG7 2RD, England

^bCentro de Astrofísica, Universidade do Porto, Rua das Estrelas, 4150-762 Porto, Portugal

^cFaculdade de Ciências, Universidade do Porto, Rua do Campo Alegre, 4150-007 Porto, Portugal

^dDepartment of Applied Physics, Delft University of Technology, P.O. Box 5046, 2600 GA Delft, The Netherlands

^eLaboratoire de l'Accélérateur Linéaire, Université de Paris-Sud, CNRS/IN2P3, Bâtiment 200, BP 34, 91898 Orsay Cedex, France

E-mail: tavgoust@gmail.com, Carlos.Martins@astro.up.pt, mmonteiro@fc.up.pt, up110370652@alunos.fc.up.pt, gluzzi@lal.in2p3.fr

Abstract. We study cosmological models involving scalar fields coupled to radiation and discuss their effect on the redshift evolution of the cosmic microwave background temperature, focusing on links with varying fundamental constants and dynamical dark energy. We quantify how allowing for the coupling of scalar fields to photons, and its important effect on luminosity distances, weakens current and future constraints on cosmological parameters. In particular, for evolving dark energy models, joint constraints on the dark energy equation of state combining BAO radial distance and SN luminosity distance determinations, will be strongly dominated by BAO. Thus, to fully exploit future SN data one must also independently constrain photon number non-conservation arising from the possible coupling of SN photons to the dark energy scalar field. We discuss how observational determinations of the background temperature at different redshifts can, in combination with distance measures data, set tight constraints on interactions between scalar fields and photons, thus breaking this degeneracy. We also discuss prospects for future improvements, particularly in the context of Euclid and the E-ELT and show that Euclid can, even on its own, provide useful dark energy constraints while allowing for photon number non-conservation.

Contents

1	Introduction	1
2	CMB Temperature Evolution	2
3	Links to varying alpha	4
4	Links to dark energy	8
5	Constraints from current data	12
6	Constraints from future datasets	16
7	Conclusions	18

1 Introduction

The observational evidence for the acceleration of the universe demonstrates that our canonical theories of gravitation and particle physics are incomplete, if not incorrect. A new generation of ground and space-based astronomical facilities (most notably the E-ELT and Euclid) will shortly be able to carry out precision consistency tests of the standard cosmological model and search for evidence of new physics beyond it.

After a quest of several decades, the recent LHC detection of a Higgs-like particle [1, 2] finally provides strong evidence in favour of the notion that fundamental scalar fields are part of Nature’s building blocks. A pressing follow-up question is whether the associated field has a cosmological role, or indeed if there is another cosmological counterpart. If there is indeed a cosmologically relevant scalar field, the natural expectation is for it to couple to the rest of the degrees of freedom in the model, unless there are symmetry principles suppressing these couplings. Therefore, not allowing for such couplings may significantly bias the analysis of current and future cosmological datasets.

In this paper, which is a sequel to [3], we focus on potentially observable signatures of the interaction of cosmological scalar fields with the electromagnetic sector, specifically changes to the standard evolution of the Cosmic Microwave Background temperature with redshift,

$$T(z) = T_0(1 + z). \quad (1.1)$$

Rather than focusing on a particular favoured model and obtaining specific constraints, we consider two general classes of models from the Cosmology literature, described in a phenomenological way. These include models in which a scalar field drives variations of the fine-structure constant, and models where the scalar field is responsible for cosmic acceleration. Since scalars can in general couple to the electromagnetic sector, our goal is to demonstrate that such scalar-photon couplings, if not accounted for, can strongly bias cosmological parameter determination. We quantify how important an effect these couplings can have on constraints derived from current and future datasets, and show how the degeneracy can be broken through the independent reconstruction of the CMB temperature evolution.

The two canonical ways to reconstruct the evolution of the CMB temperature with redshift rely on spectroscopy of molecular/ionic transitions triggered by CMB photons [4–6] and on the thermal Sunyaev-Zel’dovich (SZ) effect towards clusters [7–10]. New sources will soon become available for measurements by the above methods, and entirely new methods for measuring $T(z)$ are also being developed, so it is timely to consider their impact on cosmology and on searches for new physics. There is also complementarity with other techniques that are now becoming available. In [3] we pointed out an important connection with distance-duality tests, allowing to strengthen constraints on models that violate photon number conservation. Such tests have a rich history starting from [11, 12], and a future more precise test will be carried out by Euclid [13].

While in [3] deviations from the standard evolution were constrained in a purely phenomenological (but nevertheless model-independent) way, here we discuss in con-

siderably more detail the possible links between $T(z)$ and two other astrophysical observables: measurements of nature’s fundamental dimensionless couplings and the equation of state of dark energy. As emphasised in [14], such joint measurements will be crucial for the next generation of cosmological experiments, which will carry out precision consistency tests of the underlying scenarios. We will base our discussion on two specific examples, ESA’s Euclid¹ [15] and ESO’s European Extremely Large Telescope (E-ELT) [16]. We find that, although for varying- α models determinations of $T(z)$ will not reach the required sensitivity in the near future, in the case of dark energy scalars, their coupling to photons can have a major effect on cosmological parameter determination but the degeneracy can readily be broken with $T(z)$ and distance measurements.

2 CMB Temperature Evolution

We start with a brief review on the redshift evolution of the CMB temperature. This is not meant to be exhaustive, but simply to introduce the basic setup we will work in. Further details can be found in the original analysis of [17], as well as in [3]. We will be assuming the presence of a canonical scalar field in an FRW background, with a \mathcal{L} agrangian

$$\mathcal{L} = \frac{1}{2}(\partial_\mu\phi)(\partial^\mu\phi) - V(\phi), \quad (2.1)$$

with

$$p_\phi = \frac{1}{2}\dot{\phi}^2 - V(\phi), \quad \rho_\phi = \frac{1}{2}\dot{\phi}^2 + V(\phi). \quad (2.2)$$

Introducing a coupling C_ϕ between the scalar field and the radiation fluid, the evolution equations for the radiation energy and number densities read

$$\dot{\rho}_\gamma + 4H\rho_\gamma = C_\phi, \quad (2.3)$$

$$\dot{n}_\gamma + 3Hn_\gamma = \Psi, \quad (2.4)$$

where Ψ depends on the coupling C_ϕ . This will in general distort the behaviour of the radiation fluid, and in particular the photon temperature-redshift relation, away from its standard evolution. Restricting our attention to the observationally relevant case of adiabatic evolution, the adiabaticity condition implies [3, 17]

$$C_\phi = \frac{p_\gamma + \rho_\gamma}{n_\gamma}\Psi, \quad (2.5)$$

and one obtains the following evolution equation for the CMB temperature

$$\frac{\dot{T}}{T} + H = \frac{\Psi}{3n_\gamma} = \frac{C_\phi}{4\rho_\gamma}. \quad (2.6)$$

¹<http://www.euclid-ec.org>

For future use, let us define a correction to the standard behaviour, $y(z)$, such that

$$T(z) = T_0(1+z)y(z), \quad (2.7)$$

and clearly $y(z) = 1$ corresponds to the standard cosmological model; we can then write

$$\frac{dy}{y} = \frac{C_\phi}{4\rho_\gamma} dt = -\frac{C_\phi}{4H\rho_\gamma} \frac{dz}{1+z}. \quad (2.8)$$

The simplest ansatz for the source term Ψ in Eqs. (2.4) and (2.6) is $\Psi = 3\beta H n_\gamma$, which yields the relation

$$T(z) = T_0(1+z)^{1-\beta}; \quad (2.9)$$

this has been fairly widely used in the past, with the available measurements of $T(z)$ providing a constraint on the parameter β [3, 6, 10]. The corresponding evolution of the radiation density is

$$\rho_\gamma \propto T^4 \propto (1+z)^{4(1-\beta)} \propto a^{-4(1-\beta)}. \quad (2.10)$$

A generalisation has been suggested by Bassett and Kunz [11]², with $\Psi = 3\beta H(1+z)^{\lambda-1}n_\gamma$ and again assuming adiabaticity. The previous case is recovered for $\lambda = 1$, while for $\lambda \neq 1$ we get

$$\rho_\gamma \propto a^{-4} \exp\left[\frac{4\beta}{1-\lambda} a^{1-\lambda}\right], \quad (2.11)$$

$$T(z) = T_0(1+z) \exp\left[\frac{\beta}{1-\lambda} \left((1+z)^{\lambda-1} - 1\right)\right]. \quad (2.12)$$

Naturally, if we linearise in β and then in redshift we recover the usual linear modification to the standard temperature-redshift relation, $T(z) = T_0[1 + (1-\beta)z]$. The dependence on λ appears at order $\mathcal{O}[\beta(\lambda-2)z^2]$.

For the scalar field energy density we have

$$\dot{\rho}_\phi + 3H(1+w_\phi)\rho_\phi = -C_\phi, \quad (2.13)$$

which, in models where the scalar field is driving cosmic acceleration, could provide a link between temperature evolution (2.7-2.8) and the properties of dark energy, as will be further discussed below. In particular, for the Bassett-Kunz parametrisation [11] for photon loss, mentioned above, $T(z)$ is given by (2.12), while for the dark energy density we have:

$$\dot{\rho}_\phi + 3H(1+w_\phi)\rho_\phi = -4\beta H a^{1-\lambda} \rho_\gamma. \quad (2.14)$$

²In the notation of [11], our β corresponds to γ and our λ corresponds to $-\alpha$.

3 Links to varying alpha

In this section we consider models in which an evolving scalar field is driving variations of the fine structure constant through its coupling to Maxwell electromagnetism. This also allows photons to be converted into scalar particles, effectively violating photon number conservation. The violation can be described by a collision functional in the Boltzmann equation, leading to an equation of the form (2.4) and modifying the temperature-redshift relation through equation (2.6). At the same time, the scalar-photon coupling affects luminosity distances in a redshift-dependent way [3], potentially providing a complementary observational channel for probing these models.

For concreteness, let us consider the Bekenstein-Sandvik-Barrow-Magueijo (BSBM) class of models [18] in which the scalar field ψ couples exponentially to the Maxwell F^2 term in the matter Lagrangian, resulting in variations of the fine-structure constant, α . In this case we have (cf. equation (2.3))

$$\dot{\rho}_\gamma + 4H\rho_\gamma = 2\dot{\psi}\rho_\gamma = C_\psi, \quad (3.1)$$

with

$$\frac{\alpha}{\alpha_0} = \exp^{2(\psi - \psi_0)}, \quad (3.2)$$

and we immediately find, assuming adiabaticity, that (cf. equation (2.6))

$$\frac{\dot{T}}{T} + H = \frac{1}{2}\dot{\psi}, \quad (3.3)$$

$$\ln\left(\frac{aT}{a_0T_0}\right) = \frac{1}{2}(\psi - \psi_0) = \frac{1}{4}\ln\frac{\alpha}{\alpha_0}, \quad (3.4)$$

leading to

$$\frac{T(z)}{T_0} = (1+z)\left(\frac{\alpha(z)}{\alpha_0}\right)^{1/4} \sim (1+z)\left(1 + \frac{1}{4}\frac{\Delta\alpha}{\alpha}\right), \quad (3.5)$$

which is of the form of equation (2.7). Equation (3.5) was derived for the specific case of exponential coupling appearing in BSBM-type models, but note that, since the relative variation $\Delta\alpha/\alpha$ is constrained observationally to be small, such a linear dependence of $T(z)$ on $\Delta\alpha/\alpha$ is a good approximation (up to a model-dependent factor of order unity allowing for a coefficient different than 1/4) for a much wider range of couplings. Thus, we can think of (3.5) as the linear term in a Taylor expansion and use this equation as a more general phenomenological relation that can be tested observationally.

Recently, Webb et al. [19] found a significant indication (at the 4.2- σ level,) for a spatial dipole in the fine structure constant, α . If this is not a hidden systematic effect, and assuming that this class of models is correct, there should also be an additional CMB temperature dipole (that is, in addition to the standard one) in the same direction of the α dipole, and with μ Kelvin amplitude. Although this is beyond the scope of the current analysis, it should be possible to disentangle this from the ‘usual’ CMB dipole. In particular, a signal of this magnitude may be of some relevance for the recently released Planck results.

Note that in the above we did not assume an explicit expression for the redshift behaviour of α . A constant non-zero $\Delta\alpha/\alpha$ would introduce a deviation from the standard temperature-redshift law which grows linearly in redshift, see equation (3.5). Given that fine-structure constant variations are constrained to be weak and that optical/UV spectroscopic measurements lie mostly in the redshift range $1 \lesssim z \lesssim 3$, taking constant $\Delta\alpha/\alpha$ would be a reasonable approach, and any signal for such variations would be a hint of new physics. However, the theory predicts that $\Delta\alpha/\alpha$ should evolve and, as observational sensitivity increases (and data at larger redshifts gradually become available), the redshift dependence should be included in a model-dependent way. Here, we initiate such an approach, aiming at capturing the increase of $\Delta\alpha/\alpha$ with redshift in a phenomenological way. Given the limited observational sensitivity we seek a one-parameter phenomenological description for the evolution of $\Delta\alpha/\alpha$. However, such a simple parametrisation can be expected to be sufficient because most current measurements are firmly in the matter era, where the evolution is simple.

Let us return to the case of BSBM discussed above. In this class of models, if one neglects the recent dark energy domination one can easily find an analytic solution (i.e., a matter era one)

$$\frac{\Delta\alpha}{\alpha} = -4\kappa \ln(1+z), \quad (3.6)$$

or in other words

$$T(z) = T_0(1+z) [1 - \kappa \ln(1+z)], \quad (3.7)$$

where κ is a dimensionless parameter to be constrained by data. Note that the logarithmic factor is of order unity in the observationally relevant redshift range, say $0.5 \lesssim z \lesssim 3$. Dark energy can easily be included numerically but, in this redshift range, it only affects the lower end near $z \sim 0.5$ by a factor of order unity. For even smaller redshifts, the effect of dark energy is to further damp down variations of α [18]. Thus, equation (3.6) is also useful more generally, as a one-parameter toy model alternative to the standard β parametrisation, which phenomenologically captures the redshift evolution of $\Delta\alpha/\alpha$ at intermediate redshifts.

In the following, we will use equation (3.7) to make contact with $T(z)$ data at redshifts of order unity. We should however first check that values of the parameter κ required to produce α variations at the level of current sensitivity are not in conflict with the atomic clock bounds at $z = 0$ [20]. Since dark energy domination at late times has the effect of damping $\Delta\alpha/\alpha$ [18], taking the above redshift dependence for α is conservative in that it overestimates $\Delta\alpha/\alpha$ at small redshifts. Assuming (3.6) we have

$$\frac{1}{\alpha} \frac{d\alpha}{dt} = 4\kappa H, \quad (3.8)$$

and consequently today we must have

$$\left(\frac{1}{\alpha} \frac{d\alpha}{dt} \right)_0 \lesssim 4\kappa H_0 = 1.3(\kappa h) \times 10^{-17} s^{-1}, \quad (3.9)$$

where the inequality is due to dark energy. According to Rosenband *et al.* [20] this variation is constrained to be

$$\left(\frac{1}{\alpha} \frac{d\alpha}{dt}\right)_0 = (-1.6 \pm 2.3) \times 10^{-17} \text{yr}^{-1}, \quad (3.10)$$

which corresponds to the bound

$$\kappa_{\text{clocks}} < (5.4 \pm 7.7) \times 10^{-8} \quad (3.11)$$

when the inequality in (3.9) is saturated. In practice, κ can be significantly larger due to the effect of dark energy suppressing α variations in the present era, but note that even this figure is consistent with the aforementioned dipole hint [19]: if one ignores the direction of sources on the sky and naively fits the entire dataset to the above function, there is no strong evidence for a non-zero κ . The spatial dependence of these measurements will be addressed in subsequent work. There is thus no tension with atomic clock constraints.

As discussed in [3] the typical precision expected for temperature measurements will significantly increase with the next generation of facilities. Specifically we consider ESPRESSO [21], under construction for the VLT, and the planned HIRES for the E-ELT (for which the CODEX Phase A study [22] provides a realistic benchmark); their typical expected precisions in the temperature measurements are respectively

$$\Delta T_{\text{Espresso}} \sim 0.35 \text{ K} \quad (3.12)$$

and

$$\Delta T_{\text{Hires}} \sim 0.07 \text{ K}. \quad (3.13)$$

These are about three orders of magnitude larger than what one would expect the temperature variation to be in the BSBM model at $z \sim 4$, on the assumption that the Webb detection is correct. To get an intuitive picture of the sensitivity of $T(z)$ measurements within this class of models, one can determine what would be the smallest value of κ detectable by *a single measurement* by those two future spectrographs. This result is shown in Fig. 1, giving then a detection limit around $\kappa = 0.004$ for HIRES and $\kappa = 0.02$ for ESPRESSO.

However, these sensitivities will rapidly improve. Note that the detection limits shown in Fig. 1 are for a single measurement and they also depend on the redshift at which the measurements are made: the higher the redshift, the stronger the constraints that can be achieved. Clearly a detection of a Webb-level value of κ would require a very large number of sources, which are not currently known. However, this may be possible for clusters (whose expected sensitivity in the case of Planck is also depicted): even though they are at much lower redshifts (when deviations from the standard behaviour are correspondingly smaller), samples of thousands of clusters are expected to become available very soon. This is further discussed in [3, 23].

Recently Muller *et al.* [24] have provided the very tight measurement $T = (5.08 \pm 0.10)$ K at $z = 0.89$, using radio-mm molecular absorption measurements.

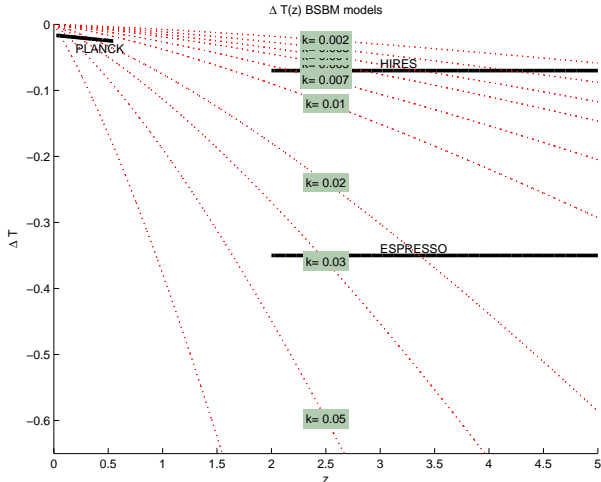


Figure 1. Variation of the temperature (relative to the standard model) as function of redshift in a BSBM-like class of models, for different values of κ and using $T_0 = (2.725 \pm 0.002)$ K. Also depicted are the limits of detection of this difference with CODEX/HIRES, ESPRESSO and Planck clusters [3]. The span of each bar is meant to represent the typical redshift range of each set of measurements.

With the ALMA array [25] gradually becoming available, the number and quality of these measurements will steadily increase, although they will be time-consuming and there will be strong competition for ALMA observing time. Nevertheless this method offers the exciting prospect of a new tool to map $T(z)$ over a very wide redshift range, potentially up to $z = 6.5$ (J. Black, private communication).

One can also check agreement with the Oklo natural nuclear reactor bound (corresponding to an effective redshift $z = 0.14$), which is

$$\frac{\Delta\alpha}{\alpha} = (0.6 \pm 6.2) \times 10^{-8} \quad (3.14)$$

according to Petrov *et al.* [26], or

$$\frac{\Delta\alpha}{\alpha} = (0.7 \pm 1.8) \times 10^{-8} \quad (3.15)$$

according to Gould *et al.* [27]; this does happen, but in any case there are several caveats with interpreting these Oklo analyses. The most obvious one is that the nuclear reactions being considered are mostly sensitive to the strong nuclear coupling, so assuming that only the fine-structure constant α varies while the rest of the physics is unchanged is a naive assumption. At higher redshifts, an additional consistency test will be provided by the redshift drift measurements carried out by high-resolution spectrographs like HIRES [14, 28].

Let us now explore the relation of these measurements with independent determinations of distance measures, in the context of the varying- α models we are considering.

In [3] we have shown that if the temperature-redshift relation is changed to

$$T(z) = T_0(1+z)y(z) \quad (3.16)$$

in models where photon number is not conserved, then the distance duality relation is correspondingly affected:

$$d_L(z) = d_A(z)(1+z)^2 y(z)^{3/2}, \quad (3.17)$$

where d_L and d_A are the luminosity and angular diameter distance measures respectively. Therefore for this class of varying- α models we predict that

$$\begin{aligned} d_L(z) &= d_A(z)(1+z)^2 \left(\frac{\alpha(z)}{\alpha_0} \right)^{3/8} \sim d_A(z)(1+z)^2 \left(1 + \frac{3}{8} \frac{\Delta\alpha}{\alpha} \right) \\ &\sim d_A(z)(1+z)^2 \left[1 - \frac{3}{2} k \ln(1+z) \right]. \end{aligned} \quad (3.18)$$

Again, this relation can be tested for both time and/or spatial variations of α ; even though the effect is small, there are hundreds (and in the future there will be thousands) of type Ia supernova measurements. Recently [29] found a 2σ hint for a ‘supernova dipole’ aligned with the α dipole. Their analysis does not take into account the effects of varying α on the supernova brightness (see [30] for a succinct discussion). Such effects are negligible with current supernova sensitivities but they could soon become relevant as datasets of a few thousands of supernovae became available. It would be very interesting to include these effects in a fully consistent analysis.

There are therefore a number of consistency tests for this class of models, involving on the one hand astrophysical measurements of T and α , and on the other hand distance measurements such as d_L .

4 Links to dark energy

We now move to studying models in which a scalar (or pseudo-scalar) field is responsible for dark energy, but also couples to the electromagnetic sector. This can happen for example through an axion-like ‘F-F dual’ coupling. Unlike the case of varying- α models, where we found that current constraints on α -variation imply that the scalar-photon coupling has a negligible effect on current data interpretation (but could soon become significant), in the case of dark energy we will see that, consistent with current constraints, scalar-photon couplings can have a major impact on cosmological data determinations and must therefore be included in data analyses. In particular, the photon-number violation induced by the scalar-photon interactions can significantly affect luminosity distances and has an important effect on cosmological analyses that include supernova data. However, independent measurements of $T(z)$ can be readily used to break this degeneracy.

Let us consider a cosmological model in which a scalar field ϕ is responsible for dark energy, but also couples to photons. The coupling involves two photons and a

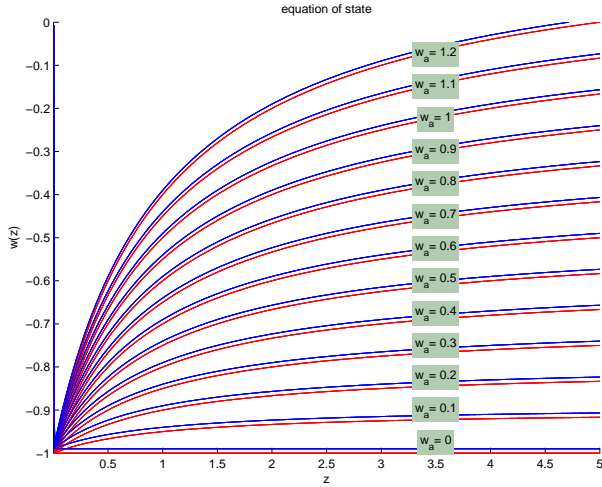


Figure 2. The equation of state of dark energy as a function of redshift for different values of the parameters w_0 and w_a . For each pair of curves the bottom (red) one corresponds to the case $w_0 = -1$ and the top (blue) one to $w_0 = -0.99$.

scalar particle and allows, for example, a scalar particle to convert into a photon in the presence of a magnetic field. Instead of considering a particular model and studying its equations of motion, we will describe this effect in a phenomenological way. Our goal is not to study any given model or exhaust all possibilities, but instead to demonstrate that such couplings can have a significant effect on cosmology.

The decay of the scalar field can be effectively described in the scalar field fluid equation through a term proportional to the scalar energy density. We parametrise this as

$$\dot{\rho}_\phi + 3H(1 + w_\phi)\rho_\phi = -3kH\rho_\phi, \quad (4.1)$$

where the parameter k (to be constrained) depends on the intergalactic magnetic field.

For our present purpose we need to adopt a specific dark energy parametrisation, so we shall take the simple and well-known Chevallier-Polarski-Linder (CPL) one [31]

$$w_\phi(a) = w_0 + w_a(1 - a). \quad (4.2)$$

Figure 2 shows the behaviour of this equation of state for different values of the parameters w_0 and w_a , chosen so as to have an equation of state close to -1 at $z = 0$ and between 0 and -1 at a redshift of $z = 5$. More specifically, we have taken $w_0 = -0.995 \pm 0.005$ and $w_a = 0.6 \pm 0.6$.

In this case the scalar field energy density evolves as

$$\rho_\phi(a) = \rho_{\phi 0} a^{-3(1+w_0+w_a+k)} \exp[-3w_a(1-a)]; \quad (4.3)$$

in other words the coupling produces an effective correction to the CPL equation of state

$$w_{\text{eff}}(a) = w_{\text{CPL}}(a) + k. \quad (4.4)$$

It follows that within the context of this class of models we can use $T(z)$ measurements to impose constraints on the dark energy equation of state parameters w_0 and w_a , as well as on the coupling k . This has already been done in two papers by Jetzer & Tortora [32, 33], although there it was done for a specific and somewhat unrealistic decaying-lambda model.

If the scalar only couples to radiation (couplings to matter are very strongly constrained), then energy conservation implies that for the radiation component we have

$$\dot{\rho}_\gamma + 4H\rho_\gamma = 3kH\rho_\phi. \quad (4.5)$$

Note that this is of the form (2.3) with $C_\phi = 3kH\rho_\phi$. In this case the evolution equation for the CMB temperature, written in terms of the correction term y defined in (2.7), is as follows

$$\frac{dy}{y} = \frac{3k}{4} \frac{\rho_\phi}{\rho_\gamma} \frac{da}{a}. \quad (4.6)$$

We can then substitute ρ_ϕ by the expression above, while for ρ_γ we have $\rho_\gamma \propto T^4$. The resulting differential equation for y is not in general analytically integrable, but we can write it as

$$y^4(a) = 1 + 3k \frac{\Omega_{\phi 0}}{\Omega_{\gamma 0}} \int_1^a x^{-3(w_0+w_a+k)} \exp[-3w_a(1-x)] dx, \quad (4.7)$$

which may be integrated numerically. Equation (4.7) provides an important observational link between the dark energy equation of state and the photon temperature evolution.

We can obtain analytic approximations in two useful particular limits. First, for a constant equation of state (that is, $w_a = 0$) and assuming a small k we have

$$y^4(a) \simeq 1 + \frac{3k}{1-3w_0} \frac{\Omega_{\phi 0}}{\Omega_{\gamma 0}} [a^{1-3w_0} - 1], \quad (4.8)$$

which corresponds to

$$T(z) \simeq T_0(1+z) \left[1 + \frac{3k}{4(1-3w_0)} \frac{\Omega_{\phi 0}}{\Omega_{\gamma 0}} [(1+z)^{-1+3w_0} - 1] \right]. \quad (4.9)$$

The second (and more specific) limiting case corresponds to small redshifts, $z \ll 1$; here it is convenient to first change variables, integrating in redshift rather than the scale factor, that is

$$y^4(z) = 1 - 3k \frac{\Omega_{\phi 0}}{\Omega_{\gamma 0}} \int_0^z (1+x)^{3(w_0+w_a+k)} \exp\left[-3w_a \frac{x}{1+x}\right] \frac{dx}{(1+x)^2}. \quad (4.10)$$

We can now linearise the integral and then integrate, finding

$$y^4(z) \simeq 1 - 3k \frac{\Omega_{\phi 0}}{\Omega_{\gamma 0}} z + \mathcal{O}(z^2), \quad (4.11)$$

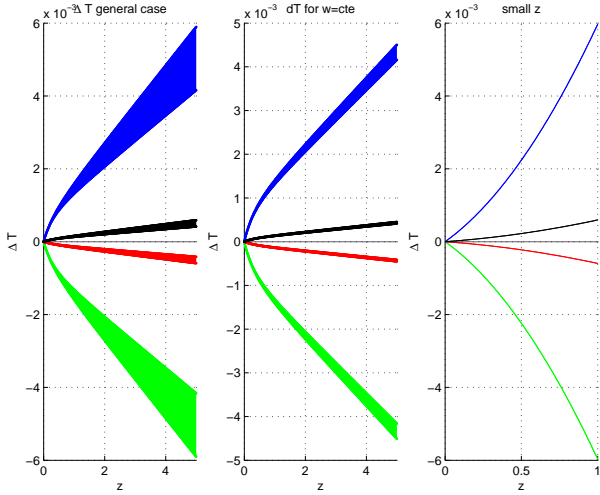


Figure 3. Deviation of the temperature relative to the standard model as a function of redshift for the general equation (left), the constant equation of state limit (middle) and the small redshift approximation (right) for different values of the parameters w_0, w_a and k . From top to bottom each set of curves respectively corresponds to $k = -10^{-7}$, $k = -10^{-8}$, $k = 10^{-8}$ and $k = 10^{-7}$ respectively; in each case, the corresponding band spans the range of w_0 and w_a discussed in the main text. Note that the small- z approximation is only accurate until about $z \sim 0.05$.

which corresponds to

$$T(z) \simeq T_0(1+z) \left(1 - \frac{3k}{4} \frac{\Omega_{\phi 0}}{\Omega_{\gamma 0}} z \right). \quad (4.12)$$

Interestingly, at first order this just depends on k , and not on w_0 (a w_0 dependency does exist at second order).

Figure 3 shows the deviation of the temperature relative to the standard model as a function of redshift for the general case (left), the constant equation of state case (middle) and for the small redshift approximation (right). Given the sensitivities discussed in the previous section, for this parametrisation HIRES will be precise enough to constrain this type of models.

Notice that for sufficiently large values of k (in absolute value) one must have k negative, otherwise the sign of the $y(z)$ factor can change. One can thus infer the prior range of k (as a function of w_0) so as to have $y(z)$ non-negative for all redshifts. For the simplest case with $w_a = 0$ and with typical values of the other relevant parameters, we find the approximate bound

$$k < 5h^{-2} \times 10^{-5}. \quad (4.13)$$

In the case of the small redshift approximation (assumed, quite optimistically, to hold up to redshift $z \sim 1$) the temperature evolution does not depend on w_0 , and one immediately finds a limiting value of $k_{max} < 10^{-6}$. Another way to set a rough prior range for k is to check whether or not the temperature reaches 3000K in the modified

equations. These considerations place k at values too small to make a significant contribution on the effective equation of state of dark energy in equation (4.4). However, the effect of k on the temperature evolution, equation (4.7), can be large as it is enhanced by the factor $\Omega_{\phi 0}/\Omega_{\gamma 0}$. As we will see in the next section, the corresponding effect on luminosity distances for values of k at this level can be very large.

As before, it is useful to get an intuitive idea for the sensitivity of $T(z)$ measurements on the dark energy equation of state in this class of scalar field models. Assuming that $w_a = 0$ and the present matter density of the universe is known, we find that a set of ESPRESSO $T(z)$ measurements could on its own constrain w_0 to a precision $\delta w_0 \sim 0.4$, while a HIRES-like spectrograph can reach $\delta w_0 \sim 0.15$; these numbers apply for an optimistic choice of fiducial model with $k \sim -10^{-5}$. (Note that these constraints are weaker than those found by [32, 33], but that's due to the fact that these authors are assuming a specific model where w_0 and k are not independent, i.e. they have a single free parameter to constrain.) On the other hand, the analysis does not include $T(z)$ measurements from clusters or from ALMA, which will be discussed in more detail elsewhere.

As a final comment we point out that the same methods can be applied to constrain a wide range of phenomenological models of the form (2.3),(2.13). As an example, take

$$\dot{\rho}_\phi + 3H(1 + w_\phi)\rho_\phi = -4\beta H\rho_\gamma, \quad (4.14)$$

which is the particular case of Bassett and Kunz [11] for $\lambda = 1$, cf. Eq. (2.14). In this case the evolution of the radiation density and its temperature are trivially

$$T(z) = T_0(1 + z)^{1-\beta} \quad (4.15)$$

$$\rho_\gamma \propto T^4 \propto (1 + z)^{4(1-\beta)} \propto a^{-4(1-\beta)}, \quad (4.16)$$

as before, but we have more complex evolution for the dark energy density: the dark energy equation of state effectively gets a β -correction, and therefore a constraint on β may be inferred, for example, from combining type Ia supernova measurements with other distance measure determinations probing the cosmic expansion history.

5 Constraints from current data

Before discussing in more detail some prospects for the next generation of relevant observational facilities, we study the constraints that can be obtained from current data. These are already useful, even for the general case given by equations (4.3), (4.7) and (3.16).

The evolution of the dark energy density (4.3) affects cosmic expansion (predominantly at smaller redshifts $z \lesssim 1$ when dark energy starts to dominate) so all distance measures depend explicitly³ on w_0 and w_a . We can use, for example, type Ia Supernova measurements (giving $d_L(z)$), BAO (yielding $H(z)$ and $d_A(z)$), galaxy ageing (providing independent measurements of $H(z)$) and H_0 determinations. On the other hand,

³Recall that the dependence on k is negligible, as this is allowed to be at most $\sim 10^{-5}$, while w_0 and w_a range over intervals of order unity.

equations (4.7) and (3.16) have a strong dependence on k and a different dependence on w_0 , w_a , allowing degeneracies to be broken.

As was pointed out above, in the models we are considering, in which the deviation from the standard $T(z)$ relation is due to a coupling of CMB photons with the dark energy scalar field, one generally expects that the same field also couples to optical photons, thus affecting luminosity distances, as discussed in [3]. Within a given model, one can then translate $T(z)$ deviations to violations of the distance duality relation (3.17). Note that on general grounds, the coupling is expected to be weaker for lower photon frequencies, so assuming a frequency-independent coupling should yield conservative bounds on $T(z)$ violations from SN (or other optical) data.

We use the Union2.1 SNIa compilation [34] and a number of different determinations of $H(z)$: cosmic chronometers [35–37] (11 data points in the redshift range $0.1 < z < 1.75$) and the more recent [38] (8 data points at $0.17 < z < 1.1$), BAO combined with Alcock-Paczynski (AP) distortions to separate the radial component in the WiggleZ Dark Energy Survey [39] (3 data points at $z = 0.44, 0.6$ and 0.73), the SDSS DR7 BAO measurement [40] at $z = 0.35$, the BOSS BAO+AP measurement [41] at $z = 0.57$, and the recent $H(z)$ determination at $z=2.3$ from BAO in the Ly α forest of BOSS quasars [42]. This gives 25 data points in the range $0.1 < z < 2.3$.

We start with a conservative choice of (flat) priors, namely $\Omega_m \in [0, 1]$, $w_0 \in [-2.2, 0.4]$, $w_a \in [-5, 5]$ and $k \in [-5, 5] \times 10^{-5}$. For our $H(z)$ analysis, we marginalise over H_0 assuming a Gaussian prior based on the Riess et al [43] determination $H_0 = 73.8 \pm 2.4$ km/s/Mpc, while in our SN likelihoods we effectively marginalise over H_0 by marginalising over intrinsic SN brightnesses. Fig. 4 shows current constraints from combining the above luminosity distance and radial distance data on our (flat) CPL- Λ CDM models, allowing for a non-zero k in equation (4.5). The top left panel of Fig. 4 shows 2-parameter joint constraints (68% and 95%, having marginalised over k and Ω_m) for the SN (blue filled contours), $H(z)$ (dashed lines) and combined SN+ $H(z)$ data (solid line contours). Having allowed for violation of photon number conservation through the parameter k , the SN constraints on the dark energy equation of state are weak, but the constraints improve dramatically with the inclusion of $H(z)$ data that are not affected by k . The region near $w_0 = 0$, favoured (at the 1σ level) by the SN data, corresponds to negative values of k (i.e. photon dimming due to decay to scalar particles) as is evident from the top right panel of Fig. 4. The bottom left panel then shows that corresponds to large values of Ω_m , so low values for the dark energy density parameter. This is the well-known degeneracy between dark energy and photon number non-conservation, which gets broken by including the $H(z)$ data favouring Ω_m near 0.25. For comparison, in the bottom right panel we show the corresponding constraint on the $w_0 - w_a$ plane but now assuming that photon-number is conserved, $k = 0$.

In Fig. 5 we show constraints on the dark energy equation of state w for flat w CDM models, again allowing for $k \in [-5, 5] \times 10^{-5}$ (left), and enforcing photon number conservation, $k = 0$ (right). This again highlights the dramatic effect of k on constraints derived from the SN data. On the contrary, the effect of k for the $H(z)$ data is insignificant; that is, $H(z)$ alone does not significantly constrain k as mentioned

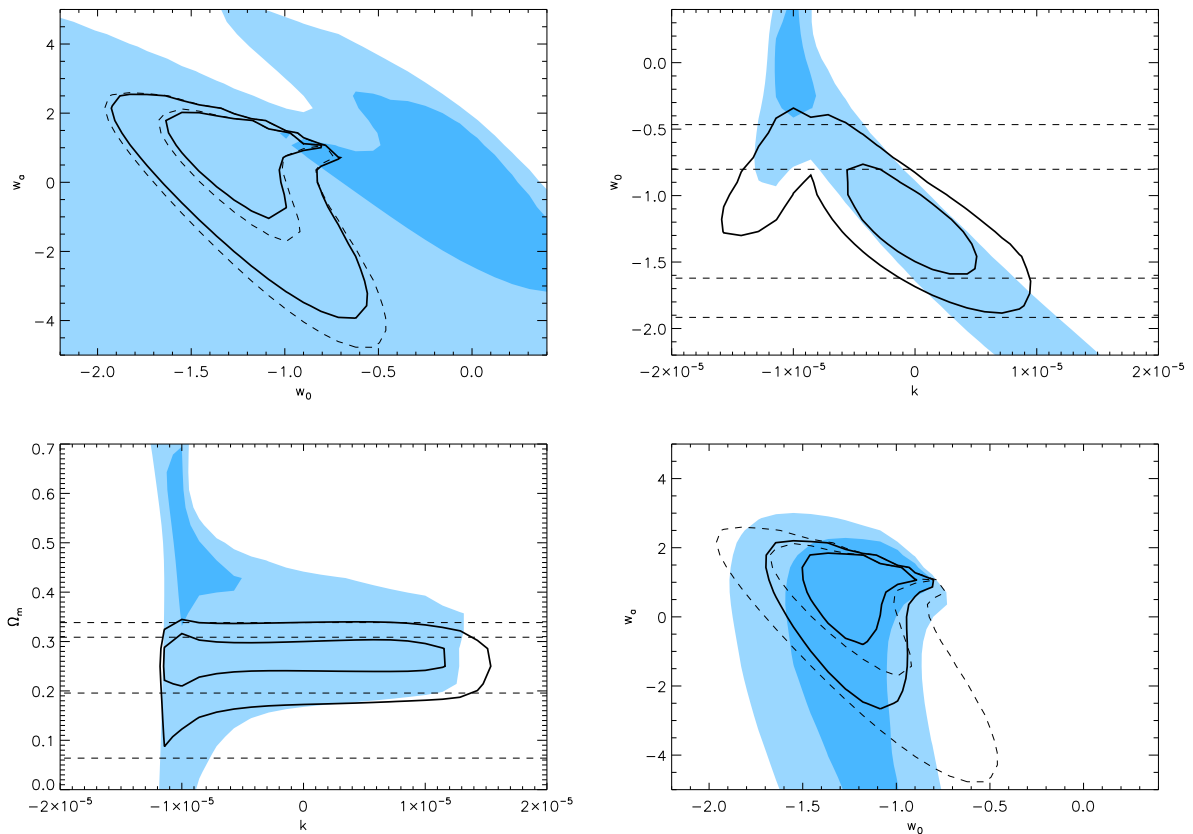


Figure 4. Current constraints on flat CPL-CDM models, allowing for violation of photon number conservation, parameterised by k . *Top Left:* 2-parameter joint constraints (68% and 95%, having marginalised over k and Ω_m) for the SN (blue filled contours), $H(z)$ (dashed lines) and combined SN+ $H(z)$ data (solid line contours). Having allowed for photon number non-conservation, the SN data alone do not strongly constrain dark energy (and favour $w_0 \sim 0$ at the 1σ level), but the inclusion of the $H(z)$ data strongly improves dark energy constraints. *Top Right-Bottom Left:* The SN data favoured region $w_0 \sim 0$ corresponds to negative k (photon dimming) and large Ω_m , exemplifying the well-known dark energy-photon dimming degeneracy. This gets broken by using the $H(z)$ data which favour $\Omega_m \simeq 0.25$. *Bottom Right:* As in top left plot but now assuming that photon-number is conserved $k = 0$. Note the dramatic effect of k on SN constraints (blue filled contours).

above—refer to equation (4.3) and the ranges of w_0 and k .

The important effect of photon-number violation on weakening SN constraints, shown in Figs. 4-5, makes clear that, in order to efficiently exploit current and future SN data for dark energy parameter determinations, one must independently constrain photon-number violations, which can be done through independent $T(z)$ determinations [3, 6, 10], as discussed above. Alternatively, one may try to shrink the SN contours by including information from other cosmological observations as priors in the marginalised parameters. Let us for example take the WMAP9+ACT+SPT+BAO+H0 result $\Omega_m = 0.263 \pm 0.015$ for the CPL-CDM model (waCDM in the WMAP data ta-

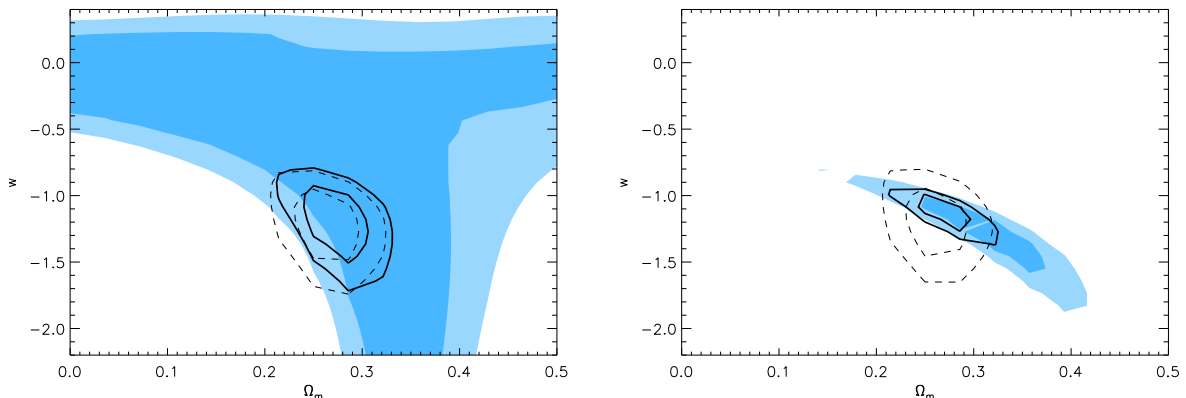


Figure 5. Left: Current constraints for flat w CDM models, allowing for violation of photon number conservation, $k \neq 0$. Right: Current constraints for flat w CDM models conserving photon-number, $k = 0$.

bles). We repeat our analysis with Ω_m still in the interval $[0, 1]$ but this time assuming a Gaussian prior (centred at 0.263 and with standard deviation 0.015) when marginalising over Ω_m . In this case, we also remove the corresponding BAO datapoints from our $H(z)$ sample (the 3 WiggleZ datapoints at $z = 0.44, 0.60$ and 0.73). The resulting constraint on the $w_0 - w_a$ plane is shown in Fig. 6. The stronger prior on Ω_m now disfavors the region with large Ω_m and negative k , thus leading to an extension of the 68% SN contour towards the region with $\{w_0 \sim -1, \Omega_m \sim 0.3, k \sim 0\}$ (also refer to Fig. 4). However, the degeneracy is not broken, and the region around $w_0 \sim 0$ is still allowed by the SN data. The overall constraint on w_0 is still controlled by the $H(z)$ data, even though the bound on w_a is now much stronger.

In the same figure, we also show the corresponding SN contours that one would obtain if k was constrained at the 10^{-5} level (dotted lines). The SN contours shrink a little, but $w_0 \sim 0$ is still allowed, and the total constraint is again controlled by the $H(z)$ data. For the Union2.1 SN dataset to become competitive with the current $H(z)$ determinations, k must be independently constrained at the $\sim 10^{-6}$ level, resulting in a SN contour similar to that of Fig 4, bottom right. This is at a level attainable using current Sunyaev-Zel’dovich $T(z)$ measurements: namely the stacked Planck SZ clusters of [44] and the constraints from SPT clusters [45]. We will present a detailed $T(z)$ analysis based both on SZ clusters and on atomic and molecular absorption lines in a follow-up publication. Such $T(z)$ constraints will therefore provide an independent means of breaking the degeneracy between dark energy parameters and photon number non-conservation, subject to completely different systematics. Currently, this degeneracy can only be broken by combining SN constraints with a k -independent dataset like $H(z)$, as we have demonstrated, and it is important to be able to also break the degeneracy by directly constraining the photon violation parameter k . Similarly, if one is instead interested in constraining photon-number violations in the context of evolving dark energy cosmologies (rather than constraining dark energy in a way that accounts for photon-number violations), then $T(z)$ measurements offer a more direct

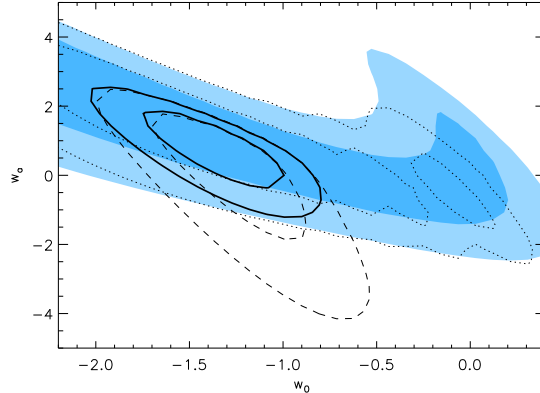


Figure 6. SN+H(z) constraints (solid line contours) on flat CPL-CDM models with a prior on Ω_m from WMAP9+ACT+SPT+BAO+H0. Blue solid contours show 68% and 95% confidence levels corresponding to the SN data, assuming a flat prior on k in the range $k \in [-5, 5] \times 10^{-5}$. For comparison, dotted line transparent contours show the corresponding constraint assuming a Gaussian prior on k centred at $k = 0$ and with $\delta k = 10^{-5}$. The dashed line contours are for H(z) data and are practically unaffected by the prior on k . For the SN-only constraints to become comparable to H(z), photon number violations must be constrained at a level $\delta k \sim 10^{-6}$.

way, complementary to standard (but indirect) distance duality analyses. Further, expected improvements in SN and H(z)/BAO data in the next decade or so may not be able to reach the desired $\delta k \lesssim 10^{-6}$ level in the context of evolving dark energy models using distance-duality methods, as we discuss in the next section.

6 Constraints from future datasets

Let us now proceed to present forecasts for future datasets. We will be particularly interested in studying the impact of the Euclid mission, and will start by considering one of its probes, BAO from the Euclid wide survey, which is expected to cover ~ 15000 deg² of extragalactic sky down to a redshift of order 2. Assuming the same conservative priors as in Fig. 4, we repeat the above analysis with simulated data for Euclid BAO and a SNAP-like SN mission. BAO radial distance errors have been estimated using the code developed by Seo & Eisenstein [46] adapted for Euclid estimated parameters [15]. For SN we follow [47] for a Dark Energy Task Force Stage IV SN mission.

The relevant constraints are shown in Fig. 7. As before, we show 68% and 95% likelihood contours for the SN data in blue (filled contours), while the transparent dashed line contours are for BAO H(z) data. The combined constraints are shown as solid line, transparent contours. Note in Fig. 7 that the constraint on w_a starts to become interesting with Euclid BAO+SNAP-like SN, even allowing for photon number non-conservation. However, in the absence of an independent constraint on k , much of the observed SN dimming can be explained by photon conversion to scalar particles,

so the SN contours grow (compared to the case $k = 0$) and the total constraint is dominated by $H(z)$.

To highlight this point, we also show in the middle and bottom left panels (dotted, transparent contours) the SN constraints achievable if the photon number violation parameter, k , could be constrained at the level 10^{-6} . This can be seen to have an important effect on the joint contours, as the SN-only constraints become competitive to the $H(z)$ -only ones. Note, in particular, that the horizontal band around $w \gtrsim 0$ (bottom left plot) for the SN data disappears, as it corresponds to a region with $k \simeq -10^{-5}$ (cf. top plots). The main message arising from this analysis is that constraining k at a level $\lesssim 10^{-6}$ will rule out this region, shrinking the SN contours by a factor of a few and improving the joint SN+ $H(z)$ constraint by a factor of ~ 2 in the context of CPL-CDM models (Fig. 7, middle left plot). We will discuss current and future constraints on k from $T(z)$ measurements, and their quantitative effect on dark energy parameter bounds, in a follow-up publication. In the rest of this section we will examine the ability of future BAO and SN surveys to jointly constrain dark energy parameters and k in the absence of such an independent bound on k .

It has been proposed that Euclid carries out a dedicated SN survey, which could yield up to a few thousand SNeIa up to redshift 1.5 [48]. This makes Euclid an ideal instrument to constrain the models we are studying, capable of delivering both radial/angular diameter distance measurements and luminosity distances, and thus minimising systematics. Based on the recently studied 6-month ‘AAA’ Euclid survey [49], one can expect more than 1700 SNe Ia in the redshift range $0.75 < z < 1.55$. We adopt the assumptions in this study and repeat our forecast analysis, now using only Euclid for both BAO and Supernovae. (We neglect the correlation between errors in different redshift bins; the effects of doing this are expected to be relatively small, given the other approximations we are also making.) Our results are shown in Fig. 8 showing that Euclid can, even on its own, provide useful constraints on Dark Energy allowing for photon number non-conservation, especially for w CDM models. Note however, that the SN-only constraints (blue filled contours) are weak and the joint constraint is dominated by the BAO $H(z)$. Further, photon-number violations, parametrised by k , cannot be constrained in this prior range by Euclid alone. Naturally, these constraints become much stronger by combining the Euclid SN with a low-redshift sample, e.g. from a SNAP-like mission (Fig. 9).

Supernova measurements with Euclid (or SNAP), can only reach a maximum redshift of around $z \sim 1.7$. However, the next generation of ground and space-based optical-IR telescopes will significantly extend this redshift range, which will bring about significant improvements in terms of dark energy constraints. Specifically, JWST (through NIRcam imaging), should find about 50 supernovae and measure their light curves [50], and with E-ELT spectroscopy provided by HARMONI [51] the redshift and supernova type can be confirmed. The redshift range of this high- z sample is expected to be $1 < z < 5$. The redshift distribution of these supernovae is not easy to extrapolate, since even the most detailed current studies such as those of the SNLS team [52] only reach out to $z \sim 1$. In the absence of a specific redshift distribution, we will simply assume it to be uniform in the above range. With these assumptions, our

Dataset	δw_0	δw_a	$\delta \Omega_m$	δk ($2\text{-}\sigma$)
Current (weak)	0.25	1.3	0.06	10^{-5}
Current (strong)	0.22	0.65	0.06	10^{-5}
Euclid(BAO)+SNAP	0.15(0.35)	0.4(1.6)	0.03	1.1×10^{-5}
Euclid only (BAO+SN)	0.15(0.35)	0.6(1.6)	0.03	—
Euclid(BAO+SN)+SNAP	0.14(0.35)	0.4(1.5)	0.025	9×10^{-6}
Euclid(BAO)+SNAP+E-ELT	0.13(0.3)	0.4(1.45)	0.023	8×10^{-6}
Euclid(BAO)+SNAP+TMT	0.13(0.25)	0.4(1.3)	0.024	8×10^{-6}

Table 1. $1\text{-}\sigma$ ($2\text{-}\sigma$) uncertainty in the relevant model parameters, marginalising over the others, for the various datasets discussed. The uncertainty quoted for the photon-number violation parameter, δk , is at $2\text{-}\sigma$. These constraints on dark energy parameters will become much stronger if k is independently constrained by an external dataset, e.g. from $T(z)$ determinations.

forecasts are shown in Fig. 10. For comparison, we also consider the alternative case of the TMT (also with JWST support) [53], which expects to find about 250 supernovae in the range $1 < z < 3$; this is shown in Fig. 11. We emphasise that the numbers we use for the E-ELT and the TMT come from assumptions made in Phase A studies of their relevant instruments; the amounts of telescope time required for gathering each dataset are not necessarily comparable.

We can see that these high-redshift supernovae lead to significantly improved constraints, compared to the previous Euclid+SNAP case. On the other hand, the constraints from the E-ELT and the TMT are comparable, indicating that the larger redshift lever arm partially compensates the smaller number of supernovae. Note, however, that these improvements on SN constraints from the inclusion of high-redshift supernovae, will only have a moderate effect on the joint BAO+SN result, unless k is independently constrained as discussed above. Table 1 provides a comparison of the uncertainties in the various model parameters obtainable in each case. Our joint analysis of future BAO+SN constraints for the various cases shows that k will only be probed at the level of $\sim 10^{-5}$ (at 95% confidence), which is below what is currently achievable using $T(z)$ measurements⁴. This also demonstrates the need to obtain independent determinations of $T(z)$, which will break the degeneracy with k , having an important effect on improving the joint constraints on dark energy parameters. We will study this in detail in a follow-up publication.

7 Conclusions

We have studied two typical classes of phenomenological scenarios involving scalar fields coupled to radiation, specifically considering their effects on the redshift evolution of the cosmic microwave background temperature. In the first of these a BSBM-type

⁴Note that the likelihood function for k has two local maxima, one at $k \simeq -10^{-5}$ and one at $k = 0$, so we do not show $1\text{-}\sigma$ errors for k in Table 1.

field provides a time variation of the fine-structure constant α , while in the other the dynamical scalar field is responsible for the recent acceleration of the universe.

Our analysis shows that the effects of the coupling of scalar fields to photons, which include effects on luminosity distances, dramatically weaken current and future constraints on cosmological parameters. In particular, our results strongly suggest that in order to fully exploit forthcoming SN data one must also independently constrain photon-number non-conservation arising from the possible coupling of SN photons to the dark energy scalar field. In this context, direct measurements of the background temperature at different redshifts (such as those provided by ALMA and HIRES) can be used in combination with distance measures to break parameter degeneracies and significantly improve constraints on physical processes in the early universe.

Nevertheless, our analysis demonstrates that Euclid can, even on its own, provide useful dark energy constraints while allowing for the possibility of photon number non-conservation. Naturally, stronger constraints can be obtained in combination with other probes. In this context it's worth emphasising that the only Euclid probes we considered are BAO and the proposed SN survey. The Euclid mission includes further probes which can be used to tighten the constraints. In this sense our results are conservative (but an analysis of this more general case is left for future work).

We have also considered the role of the increased redshift lever arm provided by type Ia supernovae at high redshift ($z > 2$), such as can be found by JWST and ground-based extremely large telescopes. Specifically, we have considered two different samples which are meant to be representative of the E-ELT and TMT, with the former going deeper into the matter era while the latter has five times more supernovae. The constraints from both datasets (in combination with lower-redshift measurements) are quite comparable: the E-ELT provides a better constraint on the matter density (for which the increased redshift lever arm is the dominant factor) while the TMT provides better constraints on the dark energy parameters w_0 and w_a (since, at least in the models we considered, dark energy is negligible at the higher redshifts, the larger number of supernovae provides the dominant effect).

Finally, let us point out that HIRES exquisite precision and stability will give it two other abilities of note: it will be able to make the first measurements of the cosmological redshift drift and also to map out the behaviour of fundamental couplings from about $z \sim 0.5$ to $z \sim 4$ and possibly well beyond. As discussed in [14, 54, 55], both of these will provide further constraints on dynamical dark energy as well as key consistency tests of many of these scenarios. Thus the combination of Euclid and the E-ELT offers us the prospect of a complete mapping of the dynamics of the dark sector of the universe all the way up to redshift $z \sim 4$, and our work highlights the point that mapping the bright sector of the universe—through $T(z)$ measurements—also plays a role in this endeavour.

Acknowledgments

This work was done in the context of the project PTDC/FIS/111725/2009 from FCT (Portugal) and the cooperation grant ‘Probing Fundamental Physics with Planck’

(PHC-EGIDE/Programa PESSOA, grant FCT/1562/25/1/2012/S), with additional support from Grant No. PP-IJUP2011-212 (funded by U. Porto and Santander-Totta). AA was supported by the Marie Curie grant FP7-PEOPLE-2010-IEF-274326 and a University of Nottingham Research Fellowship. We acknowledge useful comments and suggestions from Isobel Hook and other members of the Euclid Cosmology Theory and Transients & Supernovae Science Working Groups. We also acknowledge use of the Planck Mission Cosmological Parameters Products, which are publicly available from the Planck Legacy Archive (<http://www.sciops.esa.int/Planck>).

References

- [1] **ATLAS Collaboration** Collaboration, G. Aad *et al.*, *Observation of a new particle in the search for the Standard Model Higgs boson with the ATLAS detector at the LHC*, *Phys.Lett.* **B716** (2012) 1–29, [[arXiv:1207.7214](#)], [[doi:10.1016/j.physletb.2012.08.020](#)].
- [2] **CMS Collaboration** Collaboration, S. Chatrchyan *et al.*, *Observation of a new boson at a mass of 125 GeV with the CMS experiment at the LHC*, *Phys.Lett.* **B716** (2012) 30–61, [[arXiv:1207.7235](#)], [[doi:10.1016/j.physletb.2012.08.021](#)].
- [3] A. Avgoustidis, G. Luzzi, C. J. A. P. Martins, and A. M. R. V. L. Monteiro, *Constraints on the CMB temperature redshift dependence from SZ and distance measurements*, *JCAP* **1202** (2012) 013, [[arXiv:1112.1862](#)], [[doi:10.1088/1475-7516/2012/02/013](#)].
- [4] J. Bahcall and R. A. Wolf *Astrophys.J.* **152** (1968) [[doi:10.1086/149589](#)].
- [5] R. Srianand, P. Petitjean, and C. Ledoux, *The cosmic microwave background radiation temperature at a redshift of 2.34*, *Nature* **408** (Dec., 2000) 931–935, [[arXiv:astro-ph/0012222](#)].
- [6] P. Noterdaeme, P. Petitjean, R. Srianand, C. Ledoux, and S. López, *The evolution of the cosmic microwave background temperature. Measurements of T_{CMB} at high redshift from carbon monoxide excitation*, *A. & A.* **526** (Feb., 2011) L7, [[arXiv:1012.3164](#)], [[doi:10.1051/0004-6361/201016140](#)].
- [7] R. Fabbri, F. Melchiorri, and V. Natale *Astrophysics and Space Science* **59** (1978).
- [8] Y. Rephaeli *Astrophys.J.* **241** (1980).
- [9] E. S. Battistelli, M. DePetris, L. Lamagna, F. Melchiorri, E. Palladino, *et al.*, *Cosmic microwave background temperature at galaxy clusters*, *Astrophys.J.* **580** (2002) L101, [[arXiv:astro-ph/0208027](#)], [[doi:10.1086/345589](#)].
- [10] G. Luzzi, M. Shimon, L. Lamagna, Y. Rephaeli, M. De Petris, *et al.*, *Redshift Dependence of the CMB Temperature from S-Z Measurements*, *Astrophys.J.* **705** (2009) 1122–1128, [[arXiv:0909.2815](#)], [[doi:10.1088/0004-637X/705/2/1122](#)].
- [11] B. A. Bassett and M. Kunz, *Cosmic distance-duality as a probe of exotic physics and acceleration*, *Phys.Rev.* **D69** (2004) 101305, [[arXiv:astro-ph/0312443](#)], [[doi:10.1103/PhysRevD.69.101305](#)].
- [12] J.-P. Uzan, N. Aghanim, and Y. Mellier, *The Distance duality relation from x-ray and*

- SZ observations of clusters*, *Phys.Rev.* **D70** (2004) 083533, [[arXiv:astro-ph/0405620](#)], [[doi:10.1103/PhysRevD.70.083533](#)].
- [13] **Euclid Theory Working Group** Collaboration, L. Amendola *et al.*, *Cosmology and fundamental physics with the Euclid satellite*, *Living Rev.Rel.* **16** (2013) 6, [[arXiv:1206.1225](#)].
- [14] P. E. Vielzeuf and C. J. A. P. Martins, *Probing dark energy beyond $z = 2$ with CODEX*, *Phys.Rev.* **D85** (2012) 087301, [[arXiv:1202.4364](#)], [[doi:10.1103/PhysRevD.85.087301](#)].
- [15] R. Laureijs, J. Amiaux, S. Arduini, J.-L. Augueres, J. Brinchmann, *et al.*, *Euclid Definition Study Report*, [arXiv:Euclid Definition Study Report](#), [arXiv:1110.3193](#).
- [16] ESO, *The E-ELT Construction Proposal*, [The E-ELT Construction Proposal, document E-TRE-ESO-100-0800 Issue 2](#).
- [17] J. A. S. Lima, *Thermodynamics of decaying vacuum cosmologies*, *Phys.Rev.* **D54** (1996) 2571–2577, [[arXiv:gr-qc/9605055](#)], [[doi:10.1103/PhysRevD.54.2571](#)].
- [18] H. B. Sandvik, J. D. Barrow, and J. Magueijo, *A simple cosmology with a varying fine structure constant*, *Phys.Rev.Lett.* **88** (2002) 031302, [[arXiv:astro-ph/0107512](#)], [[doi:10.1103/PhysRevLett.88.031302](#)].
- [19] J. Webb, J. King, M. Murphy, V. Flambaum, R. Carswell, *et al.*, *Indications of a spatial variation of the fine structure constant*, *Phys.Rev.Lett.* **107** (2011) 191101, [[arXiv:1008.3907](#)], [[doi:10.1103/PhysRevLett.107.191101](#)].
- [20] T. Rosenband, D. B. Hume, P. O. Schmidt, C. W. Chou, A. Brusch, L. Lorini, W. H. Oskay, R. E. Drullinger, T. M. Fortier, J. E. Stalnaker, S. A. Diddams, W. C. Swann, N. R. Newbury, W. M. Itano, D. J. Wineland, and J. C. Bergquist, *Frequency Ratio of Al^+ and Hg^+ Single-Ion Optical Clocks; Metrology at the 17th Decimal Place*, *Science* **319** (Mar., 2008) 1808–, [[doi:10.1126/science.1154622](#)].
- [21] D. Mégevand, F. M. Zerbi, A. Cabral, P. Di Marcantonio, M. Amate, F. Pepe, S. Cristiani, R. Rebolo, N. C. Santos, H. Dekker, M. Abreu, M. Affolter, G. Avila, V. Baldini, P. Bristow, C. Broeg, P. Carvas, R. Cirami, J. Coelho, M. Comari, P. Conconi, I. Coretti, G. Cupani, V. D’Odorico, V. De Caprio, B. Delabre, P. Figueira, M. Fleury, A. Fragooso, L. Genolet, R. Gomes, J. Gonzalez Hernandez, I. Hughes, O. Iwert, F. Kerber, M. Landoni, J. Lima, J.-L. Lizon, C. Lovis, C. Maire, M. Mannelta, C. Martins, A. Moitinho, P. Molaro, M. Monteiro, J. L. Rasilla, M. Riva, S. Santana Tschudi, P. Santin, D. Sosnowska, S. Sousa, P. Spanò, F. Tenegi, G. Toso, E. Vanzella, M. Viel, and M. R. Zapatero Osorio, *ESPRESSO: the ultimate rocky exoplanets hunter for the VLT*, vol. 8446 of *Society of Photo-Optical Instrumentation Engineers (SPIE) Conference Series*, Sept., 2012.
- [22] P. Bonifacio *et al.*, *CODEX Phase A Science Case*, [CODEX Phase A Science Case, Document E-TRE-IOA-573-0001 Issue 1](#).
- [23] I. de Martino, F. Atrio-Barandela, A. da Silva, H. Ebeling, A. Kashlinsky, *et al.*, *Measuring the redshift dependence of the CMB monopole temperature with PLANCK data*, *Astrophys.J.* **757** (2012) 144, [[arXiv:1203.1825](#)], [[doi:10.1088/0004-637X/757/2/144](#)].

- [24] S. Muller, A. Beelen, J. Black, S. Curran, C. Horellou, *et al.*, *A precise and accurate determination of the cosmic microwave background temperature at $z=0.89$* , [arXiv:1212.5456](#).
- [25] M. Hogerheijde, *The ALMA Design Reference Science Plan*, *The Messenger* **123** (Mar., 2006) 20.
- [26] Y. Petrov, A. Nazarov, M. Onegin, V. Petrov, and E. Sakhnovsky, *Natural nuclear reactor Oklo and variation of fundamental constants. Part 1. Computation of neutronic of fresh core*, *Phys.Rev.* **C74** (2006) 064610, [[arXiv:hep-ph/0506186](#)], [[doi:10.1103/PhysRevC.74.064610](#)].
- [27] C. Gould, E. Sharapov, and S. Lamoreaux, *Time variability of alpha from realistic models of Oklo reactors*, *Phys.Rev.* **C74** (2006) 024607, [[arXiv:nucl-ex/0701019](#)], [[doi:10.1103/PhysRevC.74.024607](#)].
- [28] R. I. Thompson, C. J. A. P. Martins, and P. E. Vielzeuf, *Constraining cosmologies with fundamental constants - I. Quintessence and K-essence*, *M.N.R.A.S.* **428** (Jan., 2013) 2232–2240, [[arXiv:1210.3031](#)], [[doi:10.1093/mnras/sts187](#)].
- [29] A. Mariano and L. Perivolaropoulos, *Is there correlation between Fine Structure and Dark Energy Cosmic Dipoles?*, *Phys.Rev.* **D86** (2012) 083517, [[arXiv:1206.4055](#)], [[doi:10.1103/PhysRevD.86.083517](#)].
- [30] T. Chiba and K. Kohri, *Supernova Cosmology and the Fine Structure Constant*, *Prog.Theor.Phys.* **110** (2003) 195–199, [[arXiv:astro-ph/0306486](#)], [[doi:10.1143/PTP.110.195](#)].
- [31] M. Chevallier and D. Polarski, *Accelerating universes with scaling dark matter*, *Int.J.Mod.Phys.* **D10** (2001) 213–224, [[arXiv:gr-qc/0009008](#)], [[doi:10.1142/S0218271801000822](#)].
- [32] P. Jetzer, D. Puy, M. Signore, and C. Tortora, *Limits on decaying dark energy density models from the CMB temperature-redshift relation*, *Gen.Rel.Grav.* **43** (2011) 1083–1093, [[arXiv:1007.2325](#)], [[doi:10.1007/s10714-010-1091-4](#)].
- [33] P. Jetzer and C. Tortora, *Constraints from the CMB temperature and other common observational data-sets on variable dark energy density models*, *Phys.Rev.* **D84** (2011) 043517, [[arXiv:1107.4610](#)], [[doi:10.1103/PhysRevD.84.043517](#)].
- [34] N. Suzuki, D. Rubin, C. Lidman, G. Aldering, R. Amanullah, *et al.*, *The Hubble Space Telescope Cluster Supernova Survey: V. Improving the Dark Energy Constraints Above $z > 1$ and Building an Early-Type-Hosted Supernova Sample*, *Astrophys.J.* **746** (2012) 85, [[arXiv:1105.3470](#)], [[doi:10.1088/0004-637X/746/1/85](#)].
- [35] D. Stern, R. Jimenez, L. Verde, M. Kamionkowski, and S. A. Stanford, *Cosmic Chronometers: Constraining the Equation of State of Dark Energy. I: $H(z)$ Measurements*, *JCAP* **1002** (2010) 008, [[arXiv:0907.3149](#)], [[doi:10.1088/1475-7516/2010/02/008](#)].
- [36] J. Simon, L. Verde, and R. Jimenez, *Constraints on the redshift dependence of the dark energy potential*, *Phys.Rev.* **D71** (2005) 123001, [[arXiv:astro-ph/0412269](#)], [[doi:10.1103/PhysRevD.71.123001](#)].
- [37] R. Jimenez, L. Verde, T. Treu, and D. Stern, *Constraints on the equation of state of*

- dark energy and the Hubble constant from stellar ages and the CMB, *Astrophys.J.* **593** (2003) 622–629, [[arXiv:astro-ph/0302560](#)], [[doi:10.1086/376595](#)].
- [38] M. Moresco, A. Cimatti, R. Jimenez, L. Pozzetti, G. Zamorani, *et al.*, *Improved constraints on the expansion rate of the Universe up to $z = 1.1$ from the spectroscopic evolution of cosmic chronometers*, *JCAP* **1208** (2012) 006, [[arXiv:1201.3609](#)], [[doi:10.1088/1475-7516/2012/08/006](#)].
- [39] C. Blake, S. Brough, M. Colless, C. Contreras, W. Couch, *et al.*, *The WiggleZ Dark Energy Survey: Joint measurements of the expansion and growth history at $z < 1$* , *Mon.Not.Roy.Astron.Soc.* **425** (2012) 405–414, [[arXiv:1204.3674](#)], [[doi:10.1111/j.1365-2966.2012.21473.x](#)].
- [40] X. Xu, A. J. Cuesta, N. Padmanabhan, D. J. Eisenstein, and C. K. McBride, *Measuring D_A and H at $z=0.35$ from the SDSS DR7 LRGs using baryon acoustic oscillations*, [arXiv:1206.6732](#).
- [41] B. A. Reid, L. Samushia, M. White, W. J. Percival, M. Manera, *et al.*, *The clustering of galaxies in the SDSS-III Baryon Oscillation Spectroscopic Survey: measurements of the growth of structure and expansion rate at $z=0.57$ from anisotropic clustering*, [arXiv:1203.6641](#).
- [42] **BOSS Collaboration** Collaboration, N. G. Busca *et al.*, *Baryon Acoustic Oscillations in the Ly- α forest of BOSS quasars*, [arXiv:1211.2616](#).
- [43] A. G. Riess, L. Macri, S. Casertano, H. Lampeitl, H. C. Ferguson, *et al.*, *A 3Space Telescope and Wide Field Camera 3*, *Astrophys.J.* **730** (2011) 119, [[arXiv:1103.2976](#)], [[doi:10.1088/0004-637X/732/2/129](#), [10.1088/0004-637X/730/2/119](#)].
- [44] G. Hurier, N. Aghanim, M. Douspis, and E. Pointecouteau, *Measurement of the T_{CMB} evolution from the Sunyaev-Zel'dovich effect*, *A- & A.* **561** (Jan., 2014) A143, [[arXiv:1311.4694](#)], [[doi:10.1051/0004-6361/201322632](#)].
- [45] A. Saro, J. Liu, J. J. Mohr, K. A. Aird, M. L. N. Ashby, M. Bayliss, B. A. Benson, L. E. Bleem, S. Bocquet, M. Brodwin, J. E. Carlstrom, C. L. Chang, I. Chiu, H. M. Cho, A. Clochiatti, T. M. Crawford, A. T. Crites, T. de Haan, S. Desai, J. P. Dietrich, M. A. Dobbs, K. Dolag, J. P. Dudley, R. J. Foley, D. Gangkofner, E. M. George, M. D. Gladders, A. H. Gonzalez, N. W. Halverson, C. Hennig, W. L. Holzapfel, J. D. Hrubes, C. Jones, R. Keisler, A. T. Lee, E. M. Leitch, M. Lueker, D. Luong-Van, A. Mantz, D. P. Marrone, M. McDonald, J. J. McMahon, J. Mehl, S. S. Meyer, L. Mocanu, T. E. Montroy, S. S. Murray, D. Nurgaliev, S. Padin, A. Patej, C. Pryke, C. L. Reichardt, A. Rest, J. Ruel, J. E. Ruhl, B. R. Saliwanchik, J. T. Sayre, K. K. Schaffer, E. Shirokoff, H. G. Spieler, B. Stalder, Z. Staniszewski, A. A. Stark, K. Story, A. van Engelen, K. Vanderlinde, J. D. Vieira, A. Vikhlinin, R. Williamson, O. Zahn, and A. Zenteno, *Constraints on the CMB Temperature Evolution using Multi-Band Measurements of the Sunyaev Zel'dovich Effect with the South Pole Telescope*, *ArXiv e-prints* (Dec., 2013) [[arXiv:1312.2462](#)].
- [46] H.-J. Seo and D. J. Eisenstein, *Improved forecasts for the baryon acoustic oscillations and cosmological distance scale*, *Astrophys.J.* **665** (2007) 14–24, [[arXiv:astro-ph/0701079](#)], [[doi:10.1086/519549](#)].
- [47] A. Albrecht, G. Bernstein, R. Cahn, W. L. Freedman, J. Hewitt, *et al.*, *Report of the*

Dark Energy Task Force, [arXiv:astro-ph/0609591](#).

- [48] I. M. Hook, *Supernovae and Cosmology with Future European Facilities*, [arXiv:1211.6586](#).
- [49] Private communication (April 2013).
- [50] A. G. Riess and M. Livio, *The first type Ia supernovae: an empirical approach to taming evolutionary effects in dark energy surveys from SNe Ia at $z > 2$* , *Astrophys.J.* **648** (2006) 884–889, [[arXiv:astro-ph/0601319](#)], [[doi:10.1086/504791](#)].
- [51] N. Thatte, M. Tecza, F. Clarke, R. L. Davies, A. Remillieux, R. Bacon, D. Lunney, S. Arribas, E. Mediavilla, F. Gago, N. Bezawada, P. Ferruit, A. Fragoso, D. Freeman, J. Fuentes, T. Fusco, A. Gallie, A. Garcia, T. Goodsall, F. Gracia, A. Jarno, J. Kosmalski, J. Lynn, S. McLay, D. Montgomery, A. Pecontal, H. Schnetler, H. Smith, D. Sosa, G. Battaglia, N. Bowles, L. Colina, E. Emsellem, A. Garcia-Perez, S. Gladysz, I. Hook, P. Irwin, M. Jarvis, R. Kennicutt, A. Levan, A. Longmore, J. Magorrian, M. McCaughrean, L. Origlia, R. Rebolo, D. Rigopoulou, S. Ryan, M. Swinbank, N. Tanvir, E. Tolstoy, and A. Verma, *HARMONI: a single-field wide-band integral-field spectrograph for the European ELT*, vol. 7735 of *Society of Photo-Optical Instrumentation Engineers (SPIE) Conference Series*, July, 2010.
- [52] K. Perrett, M. Sullivan, A. Conley, S. González-Gaitán, R. Carlberg, D. Fouchez, P. Ripoche, J. D. Neill, P. Astier, D. Balam, C. Balland, S. Basa, J. Guy, D. Hardin, I. M. Hook, D. A. Howell, R. Pain, N. Palanque-Delabrouille, C. Pritchet, N. Regnault, J. Rich, V. Ruhlmann-Kleider, S. Baumont, C. Lidman, S. Perlmutter, and E. S. Walker, *Evolution in the Volumetric Type Ia Supernova Rate from the Supernova Legacy Survey*, *Astron.J.* **144** (Aug., 2012) 59, [[arXiv:1206.0665](#)], [[doi:10.1088/0004-6256/144/2/59](#)].
- [53] D. Silva *et al.*, *TMT Detailed Science Case*, [TMT Detailed Science Case, Document TMT.PSC.TEC.07.003 Release 01](#).
- [54] M. Martinelli, S. Pandolfi, C. J. A. P. Martins, and P. E. Vielzeuf, *Probing dark energy with the Sandage-Loeb test*, *Phys.Rev.* **D86** (2012) 123001, [[arXiv:1210.7166](#)], [[doi:10.1103/PhysRevD.86.123001](#)].
- [55] L. Amendola, A. O. Leite, C. J. A. P. Martins, N. J. Nunes, P. O. J. Pedrosa, *et al.*, *Variation of fundamental parameters and dark energy. A principal component approach*, *Phys.Rev.* **D86** (2012) 063515, [[arXiv:1109.6793](#)], [[doi:10.1103/PhysRevD.86.063515](#)].

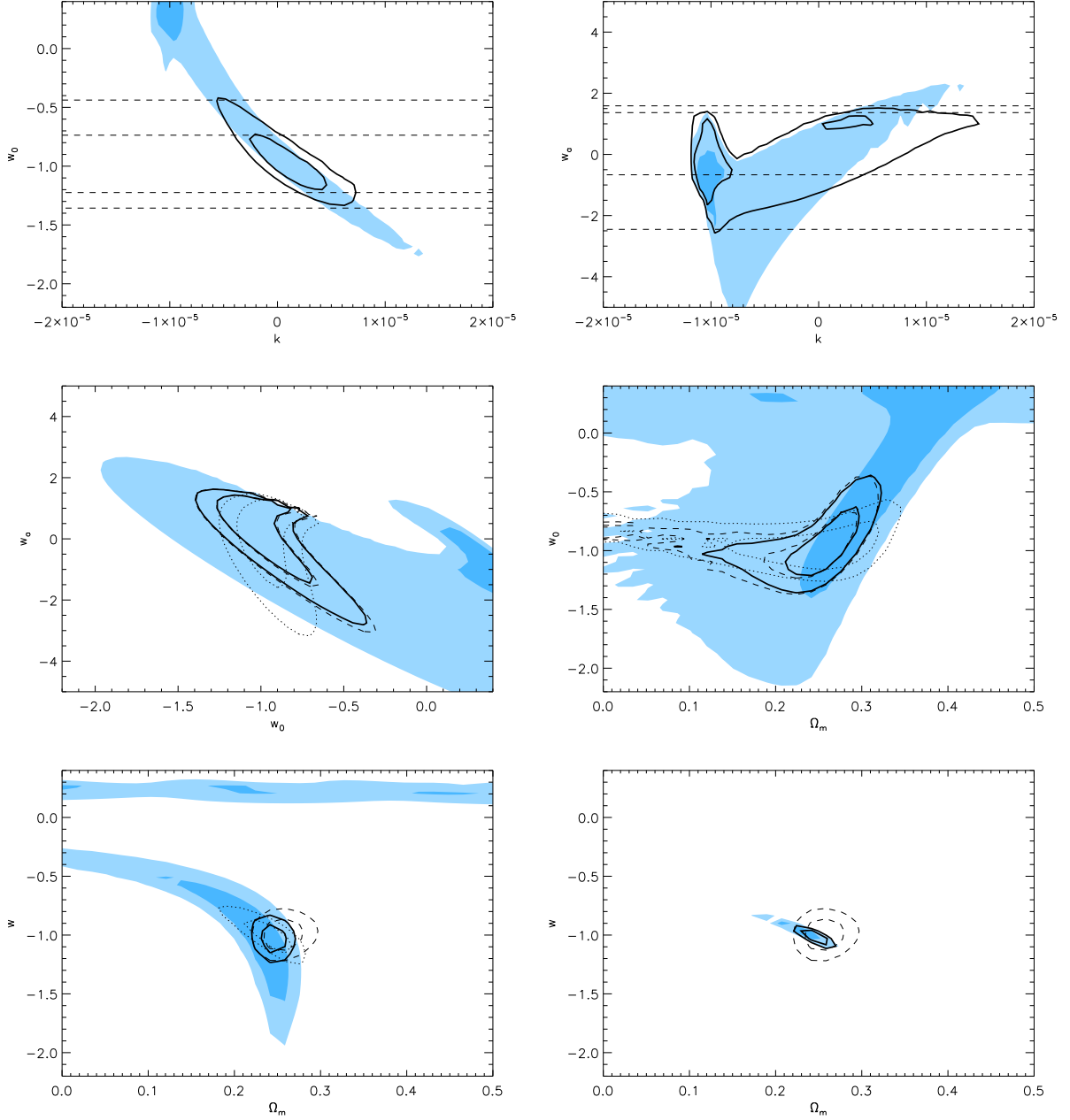


Figure 7. Forecast 68% and 95% likelihood contours for SN (filled blue), H(z) (dashed line transparent) and combined SN+H(z) (solid line transparent), considering Euclid BAO and a SNAP-like SN mission. The dotted transparent contours show the corresponding SN likelihood contours, assuming k can be constrained at the 10^{-6} level. *Top and Middle Panels:* Forecasts for flat CPL- Λ CDM models, for the conservative priors of Fig. 4. *Bottom Panel:* For comparison we show the corresponding constraints for a w CDM model for $k \in [-5, 5] \times 10^{-5}$ (left) and for $k = 0$ (right). On the left plot, note that the horizontal band around $w \gtrsim 0$ for the SN data corresponds to a region with $k \simeq -10^{-5}$ (cf. top plots), and it disappears when k is constrained at the 10^{-6} level.

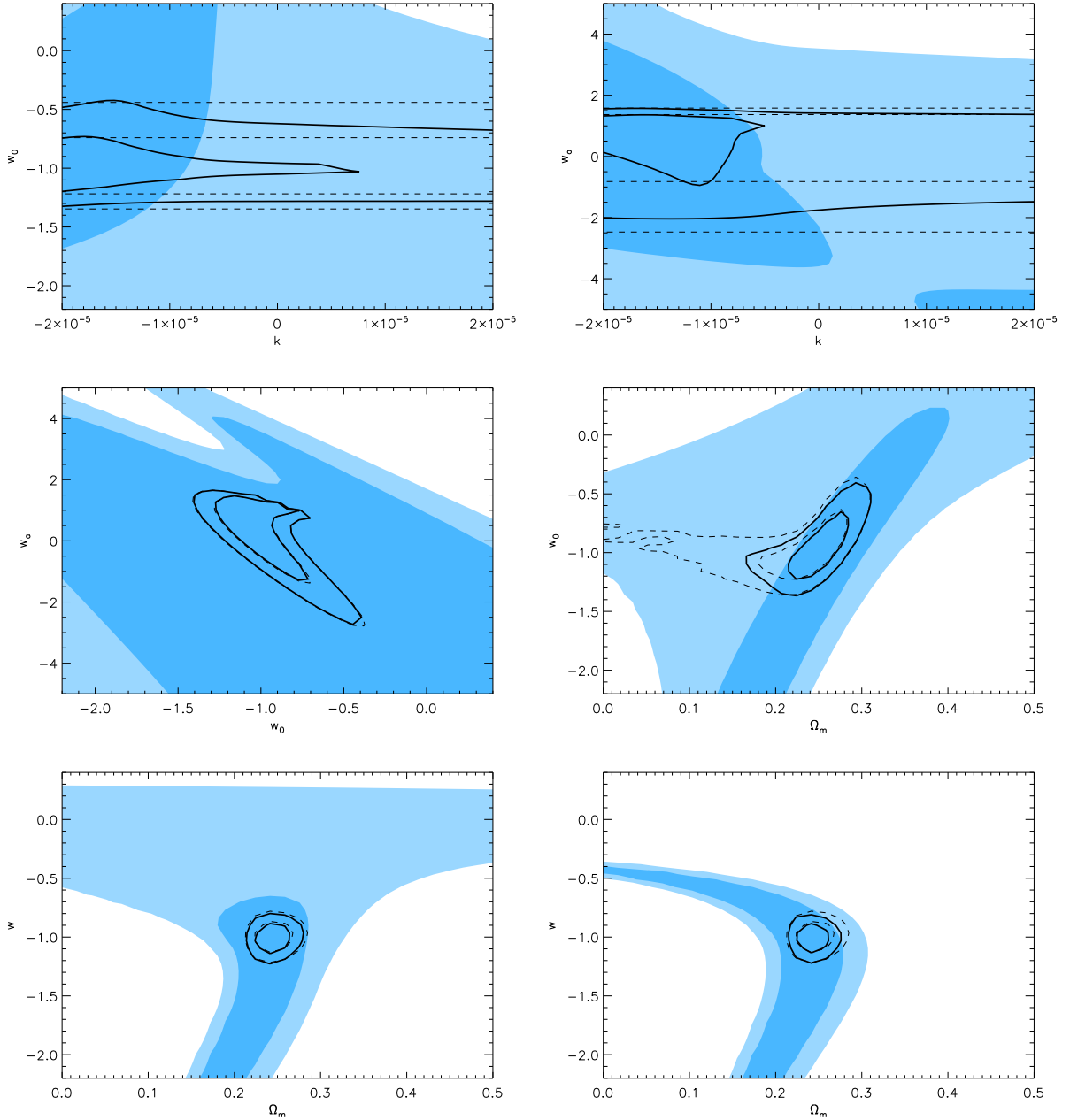


Figure 8. Forecasts for Euclid BAO (wide survey) + Euclid AAA SN survey. The plots shown are as in Fig. 7. While Euclid alone cannot strongly constrain k (violations of photon number conservation) it will still provide useful constraints on dark energy parameters, especially within the w CDM model. However, the joint constraints (solid transparent contours) are determined predominantly by the BAO data (dashed transparent contours), while the SN-only bounds (blue filled contours) are weak. Therefore, these constraints become much stronger when a low-redshift SN sample is also included, cf. Fig. 9.

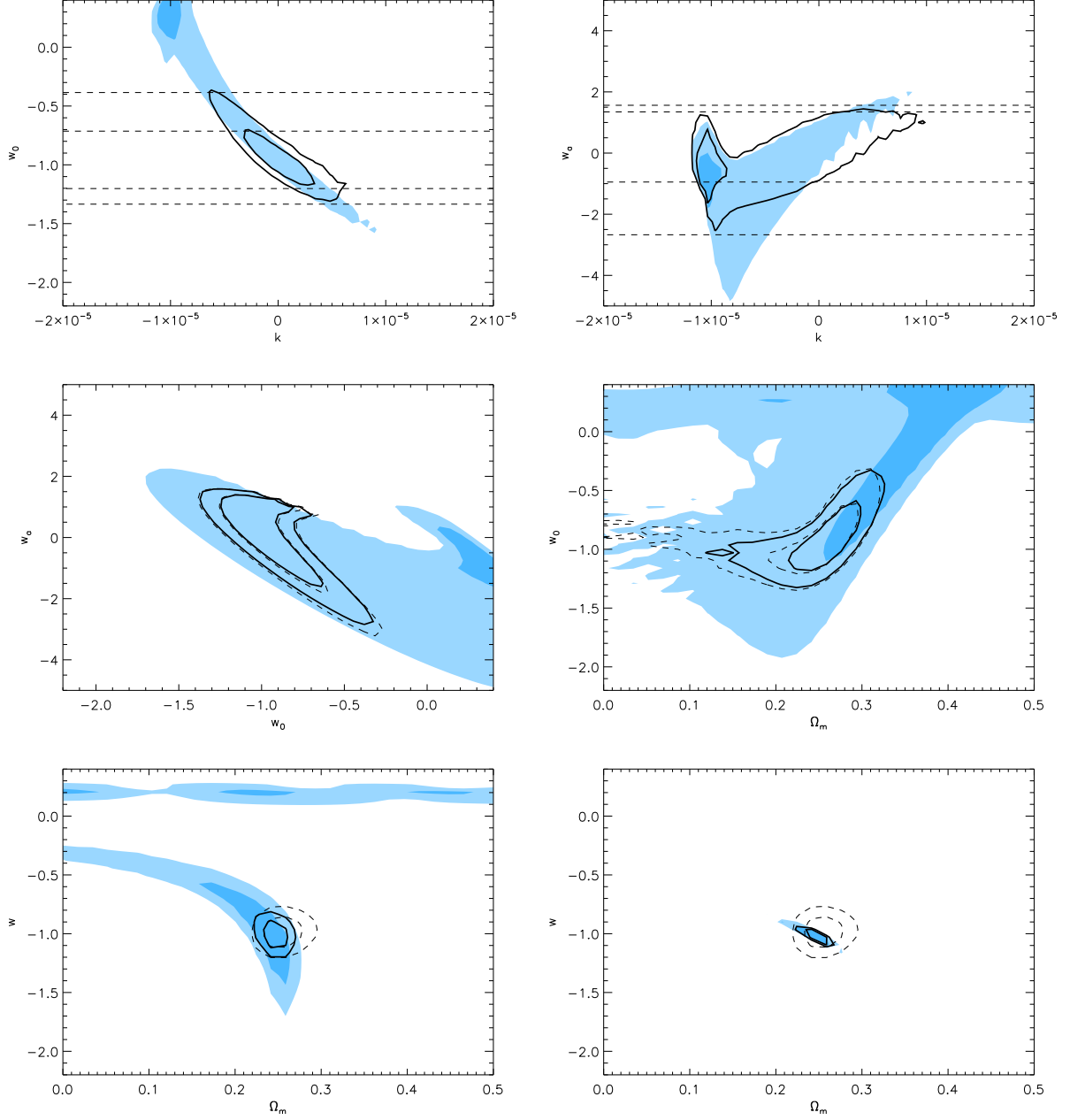


Figure 9. Forecast for Euclid (SN+BAO) combined with a low-redshift, SNAP-like sample. The combined SN constraints are now stronger (cf. Fig. 8), improving significantly the joint constraints.

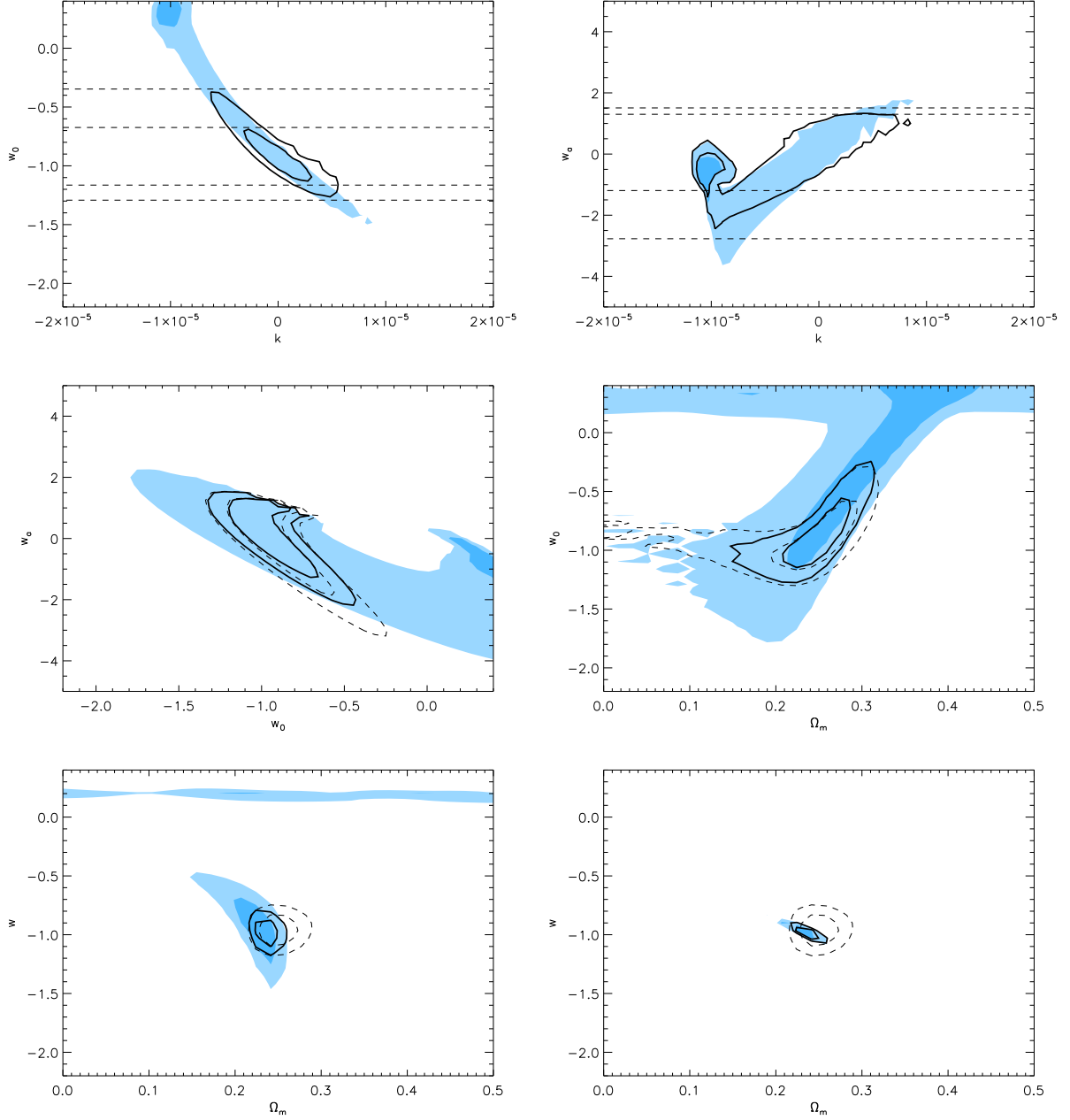


Figure 10. As above, but now showing forecasts for E-ELT combined with a SNAP-like SN mission and Euclid BAO. The additional ~ 50 SN in the range $1 < z < 5$ can lead to a significant improvement of the SN constraints.

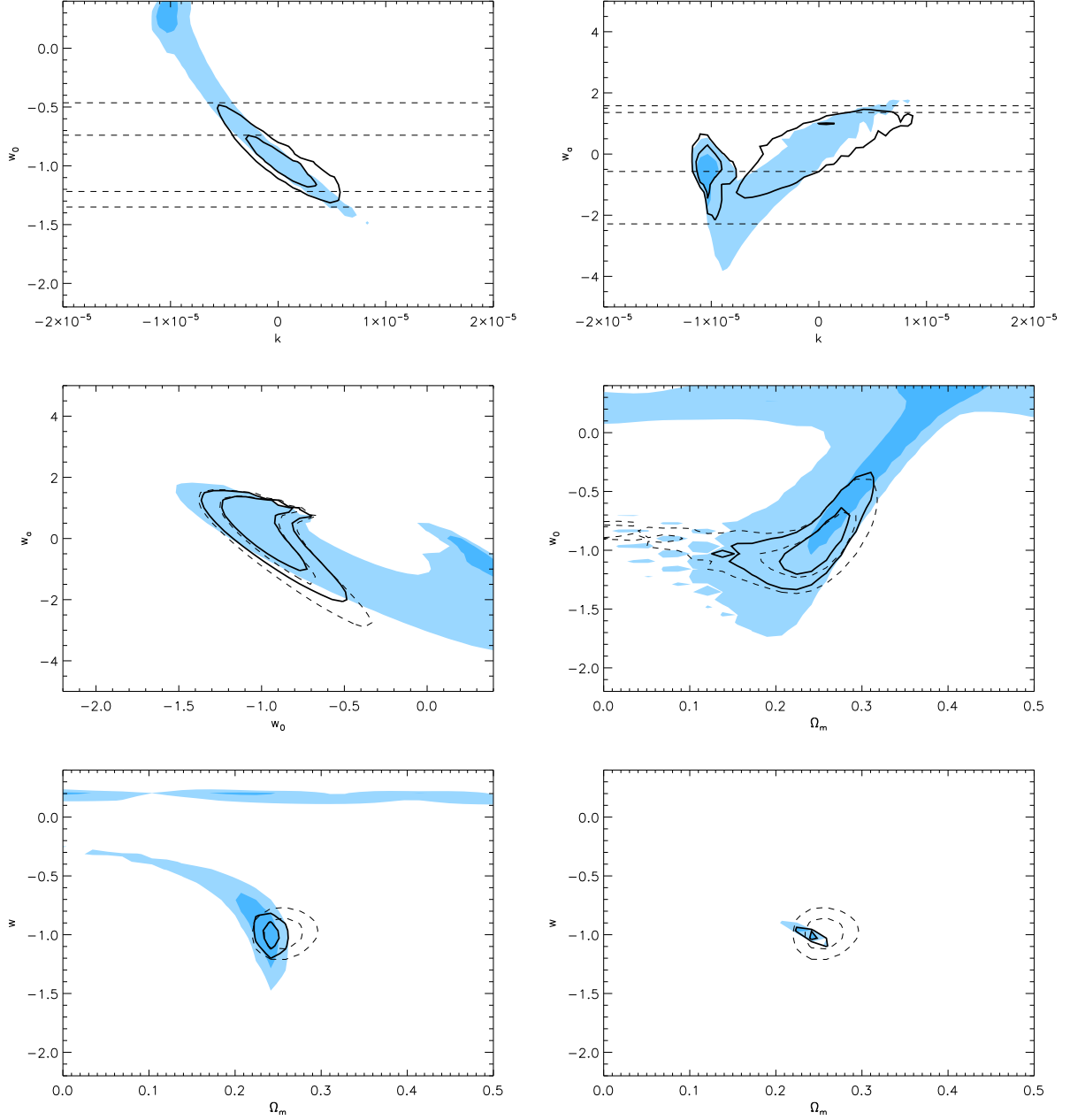


Figure 11. As above but for TMT combined with a SNAP-like SN mission and Euclid BAO. Again, the additional ~ 250 SN in the range $1 < z < 3$ would lead to a significant improvement of the SN and joint constraints.